Biomedical Signal Processing and Control 56 (2020) 101727

Contents lists available at ScienceDirect

Biomedical Signal Processing and Control

journal homepage: www.elsevier.com/locate/bspc

Enhanced EEG–EMG coherence analysis based on hand movements

Xugang Xi[a,*], Cunbin Ma[a], Changmin Yuan[a], Seyed M. Miran[b], Xian Hua[c], Yun-Bo Zhao[d], Zhizeng Luo[a,*]

[a] School of Automation, Hangzhou Dianzi University, Hangzhou, 310018, China
[b] Biomedical Informatics Center, George Washington University, Washington, DC, 20052, USA
[c] Jinhua People's Hospital, Jinhua, 321000, China
[d] Department of Automation, Zhejiang University of Technology, Hangzhou, 310023, China

ARTICLE INFO

Article history:
Received 30 June 2019
Received in revised form
26 September 2019
Accepted 13 October 2019

Keywords:
Electroencephalogram
Electromyogram
EEG–EMG coherence
Magnitude square coherence
Wavelet coherence

ABSTRACT

Electroencephalogram (EEG)–electromyogram (EMG) coherence analysis is an effective method for examining the functional connection between brain and muscles. An improved coherence approach is proposed in this study to enhance the estimation of EEG–EMG coherence. First, we sampled the synchronous EEG signal based on the burst points of the EMG signal. Then, a moving average of the sampled EEG by using a window function is performed before the EEG is sampled again on the basis of the EMG burst points. The EEG signals are reassembled to effectively reflect the muscle motions. Finally, the estimation of the EEG–EMG coherence is computed by using magnitude square coherence (MSC) and wavelet coherence. The coherence characteristics of the different autonomous movements in the β-band and γ-band are analyzed to verify the reliability of the method. Results show that our proposed method can remarkably enhance EEG–EMG coherence estimation regardless of using either MSC or wavelet coherence. The results of coherence analysis not only can correctly reflect the coupling relationship between the cortex and the muscles but can also distinguish the EEG–EMG coherences of the different autonomous movements.

1. Introduction

During the autonomous movement of the human body, the motor cortex sends out instructions to control the limbs and complete muscle movement along the motor nerve pathway through the brainstem and the spinal cord. At the same time, the limb signals are sent back to the cerebral cortex for confluence analysis along the sensory nerve conduction pathway, and instructions are transmitted to accurately complete the action. This interaction between cortex activity and muscle movement can be expressed by the coherence between the electroencephalogram (EEG) and the electromyogram (EMG). Coherence can be used in many aspects, such as in the studies of cortex–muscle function coupling and root cause of fatigue, treatment of dyskinesia, and functional rehabilitation research. Gwin [1] found that EEG–EMG coherence was higher in the γ-band during isotonic contraction, whereas EEG–EMG coherence was higher in the β- band during isometric contraction. Patino [2] found that the EEG–EMG coherences of deaf patients, as opposed to those of healthy people, were missing in the gamma bands when they performed dynamic force output tasks, which suggest that proprioception may be transmitted to the brain in the γ-band. Braun et al. [3], who required stroke patients to perform fine-grasping actions, reported that the coherence between EEG and EMG mainly appear at 10–23 Hz. Therefore, the effective analysis of EEG–EMG coherence and the comprehensive acquisition of useful information about cortex–muscle transmission both have always been popular research topics. Some studies on EEG–EMG coherence also found that although most people with dyskinesia can recover their ability to walk independently, less than 50% of them can fully recover their upper limbs [4], especially hand movements, which indicate that cortex–muscle coherence generated by hand movements is extremely important in rehabilitating patients with dyskinesia.

Some achievements have been recently achieved to describe EEG–EMG coherence, which is usually analyzed in the three aspects of time domain [5], frequency domain [6], and time–frequency domain [7]. Typical frequency–domain coherence analysis algorithms, such as magnitude square coherence (MSC) [8,9], are mainly based on the Fourier transform, in which coherence properties can be determined to a certain extent. However, performing a Fourier transform over the entire time axis cannot convey the increase of particular frequencies. A sliding window can be used

* Corresponding authors.
E-mail addresses: xixi@hdu.edu.cn (X. Xi), luo@hdu.edu.cn (Z. Luo).

https://doi.org/10.1016/j.bspc.2019.101727
1746-8094/

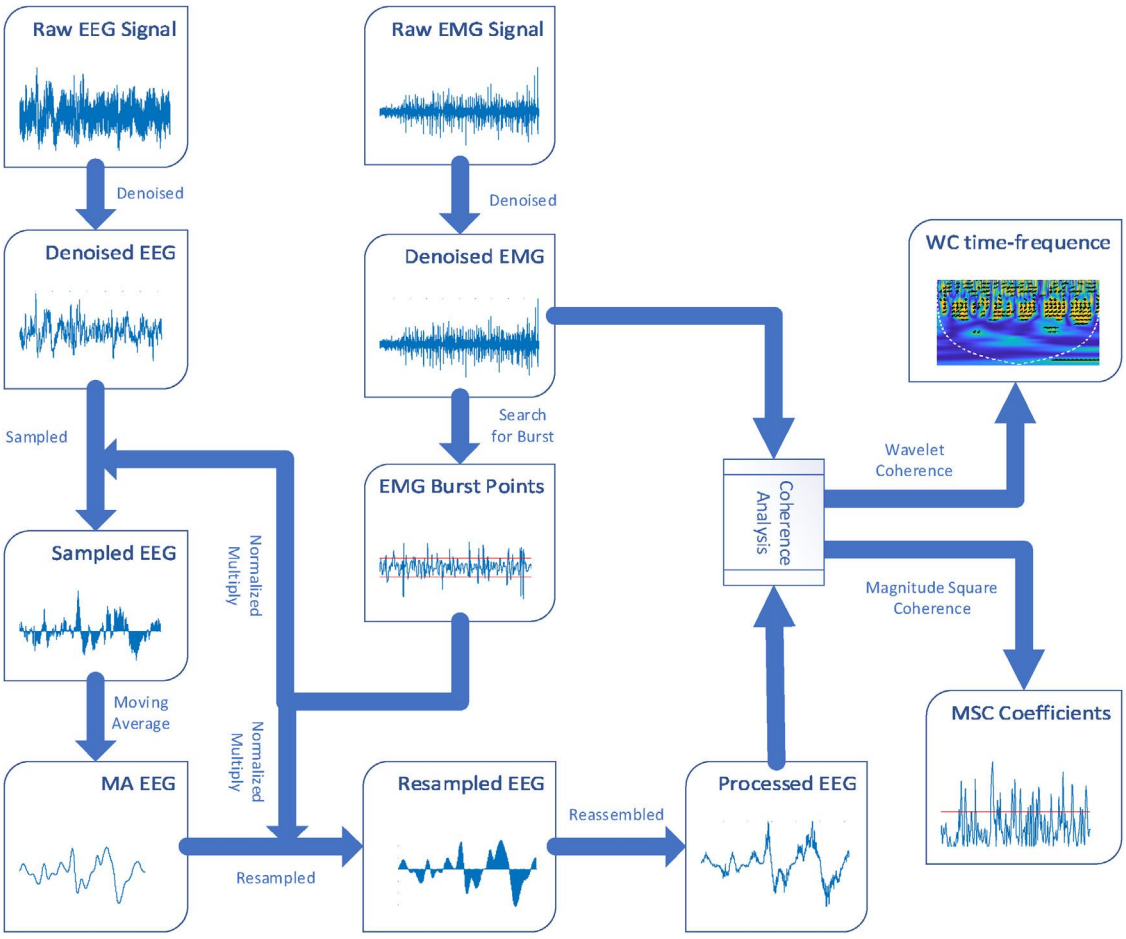

Fig. 1. Overview of the EEG–EMG coherence enhancement model.

in the short-time Fourier transform to find the spectrogram and subsequently obtain information about time and frequency [10], but the length of the window limits the resolution of the frequency. Thus, the abovementioned algorithms cannot easily take into account both time and frequency resolutions and do not consider the nonlinear characteristics of EEG and EMG. The wavelet transform can measure frequency domain characteristics at different resolutions. Time–frequency domain coherence analytical methods, such as wavelet coherence [4,11], can overcome the abovementioned issues and reflect the time–frequency local and instantaneous characteristics of nonstationary signals. On the basis of the abovementioned gaps, this study analyzes coherence based on MSC and wavelet coherence to obtain information about the cortex and the muscles under hand movements.

In the process of analyzing the coherence of EEG and EMG signals, the EEG signal is much weaker than the EMG signal in many autonomous actions, especially hand movements. Hence, the obtained values of the EEG–EMG coherence coefficients are somewhat low, which hinder the effective analysis of EEG–EMG coherence, and they influence the accuracy of the conclusions. In solving this problem, an algorithm to preprocess the synchronous EEG signal based on the most effective information of the EMG signal, which is considered to contain only the signal most related to muscle EMG activity, is proposed in this study. Then, the preprocessed EEG signal and the EMG signal are coherently analyzed in detail. The obtained estimation of the coherence is more enhanced compared with the original one, which implies that the proposed method can effectively reflect the coherent characteristics of the cortex and the muscle.

Besides, it is necessary to validate the finding by extracting relevant features of MSC coefficients and training classification to distinguish different hand movements. Some related studies have achieved some good results. Yu Zhang et al. [12] extracted temporally constrained sparse group spatial pattern (TSGSP) feature of EEG and trained the support vector machine (SVM) classifier to identify the MI tasks related hand movements. As a result, they found an acceptable classification performance. Zhichao Jin et al. [13] proposed a classification method of sparse Bayesian extreme learning machine (SBELM) to distinguish MI tasks of different hand movements, and obtained a decent classification accuracy. Yong Jiao et al. [14] applied a novel sparse group representation model (SGRM) to the classification of MI-based BCI. This method reduced the training samples of the target subject and improved the efficiency of the classification. In this study, the extracted features related to the enhanced coherence coefficients were used to train a support vector machine (SVM) and identify hand movements in comparison with the original coherence coefficients features. Finally, we discuss the advantages and the potential limitations of the algorithm and provide the future extension of the proposed method.

2. Methods and materials

2.1. Overview

Fig. 1 shows an overview of the enhanced EEG–EMG coherence approach proposed in this study. After denoising the synchronous EEG and EMG signals, EMG burst points are initially searched to

normalize EMG and derive a sampled EEG by multiplying the normalized EMG signal. Then, a Hamming window is utilized to obtain the average trend of the EEG signal by computing the moving average. Resampling EEG is performed by multiplying again the normalized EMG, and the resampled EEG signal is reassembled to derive the preprocessed EEG. Finally, MSC and wavelet coherence are computed to obtain the final results.

2.2. Enhanced EEG–EMG coherence method

EEG–EMG coherence analysis is mainly used to calculate the linear relationship of frequency domain components of EEG and EMG signals. Traditional EEG–EMG coherence is mainly based on the Fourier transform, which considers EEG and EMG signals as stationary signals for coherence analysis. In practice, the EEG signal and the EMG signal both have nonlinear characteristics. Therefore, wavelet coherence can be introduced to analyze the characteristic relationship between EEG and EMG signals. In reasonably verifying the correctness and reliability of the proposed method, this study separately adopts MSC and wavelet coherence to analyze the coherence between the EEG signals before and after preprocessing and the EMG signal.

2.2.1. EEG preprocessing based on EMG spikes

The enhanced EEG–EMG coherence can be regarded an advanced preprocessing of the EEG signal [15]. The specific algorithm involves the following:

Step 1: The collected EMG signal is denoised by the wavelet transform to obtain a pure EMG signal, as proposed in the literature [16] (Rectification is unnecessary when analyzing EEG–EMG coherence; thus, the EEG signal in the present work did not undergo rectification processing [17]). Moreover, searching for the burst points of the EMG signal is necessary and it can be implemented by identifying the peak and trough positions of the EMG signal waveforms. The peaks and troughs with small amplitudes can be removed to leave only the ones with larger amplitudes by setting certain thresholds. The arrows in Fig. 2 represent the positions of the burst points. We assume that the positional information of the burst points of the EMG signal can respond synchronously to the EEG signal more effectively when doing hand movements.

Step 2: Assume that the original EMG signal is denoised and denoted by $x(n)$. The value of 1 is set in the positions of the EMG burst points, whereas the values of the other positions are set to zero. In this manner, a new normalized EMG signal sequence $x'(n)$ can be obtained.

$$x'(n) = \begin{cases} 1, & burst\ \ occured\ \ in\ posotions\ for\ index\ n \\ 0, & other \end{cases} \tag{1}$$

Step 3: The information included in the EEG signal $x(n)$ at position n is assumed to be useful for the synchronous EEG signal, and $x(n)$ is replaced with $x'(n)$ to extract the samples of the EEG signal. The EEG samples continually repeat themselves when driving the EMG burst points. Moreover, the repeating sampled EEG signals have a constant relative position towards the EMG signal. Therefore, the EEG signal can be extracted by multiplying the EMG signal $x'(n-k)$ with time shift k to reflect its repeating characteristics. Assume that the original EMG signal denoised is $y(n)$, then

$$y(n,k) = y(n)x'(n-k),\ k = -K, \ldots, K \tag{2}$$

where K represents the maximum time shift of the synchronous EEG and EMG, in which the value is set to 4.

Step 4: The extracted EEG sample signal $y(n,k)$ contains the original EEG signal only at the bursts, and the other positions will all be zero, resulting in the scattering of the extracted sampled signals due to the presence of random noise. Therefore, in finding the repeating contributions of these sample driving signals, a window function $w(n)$ is used to compute the moving average of $y(n,k)$, which is then used to obtain a new sampled EEG signal $y'(n,k)$ with an average trend.

$$y'(n,k) = \sum_{m=-M}^{M} y(n-m,k)w(m) = y(n,k) * w(n),\ n = 1, \ldots, N \tag{3}$$

where $w(n)$ is a Hamming window with $2M+1$ weight, in which the center of the symmetry is $n=0$, N is the length of the EEG signal $y(n)$, and $*$ represents a convolution. The calculated average EEG signal can serve as an approximate of the EMG burst driving signal.

Step 5: The results of the moving average are only affected by the non-zero values in $y(n,k)$, $k=-K, \ldots, K$, and the zero values have no effect on the results. Consequently, the results obtained by computing the moving average will be non-zero, which is not conducive in reassembling $y'(n,k)$ into a new sequence. Therefore, the extraction process in step 3 is utilized again to leave the non-zero values only at the initial non-zero positions.

$$\overline{y'(n,k)} = y'(n,k)x'(n-k),\ k = -K, \ldots, K \tag{4}$$

Step 6: $\overline{y'(n,k)}$ is reassembled by adding the sequences one by one. The results are further measured by adding the coefficient a_k to obtain the final preprocessed EEG signal sequence, such that

$$y''(n) = \sum_{k=-K}^{K} a_k\, y'\overline{(n,k)}, \tag{5}$$

where a_k can be either simply ones or a Hamming window with a length of $2K+1$, in which this study finds that the latter can achieve better results.

Substituting Eqs. (2)–(4) into Eq. (5) obtains the following:

$$y''(n) = \sum_{k=-K}^{K} a_k((y(n)x'(n-k)) * w(n))x'(n-k). \tag{6}$$

The coherence estimation between $y''(n)$ (the preprocessed EEG signal) and the original denoised EMG signal $x(n)$ is computed. Results show that the values can be enhanced to a certain extent regardless of the coherence method used (i.e., either MSC or wavelet coherence).

2.2.2. Magnitude squared coherence

Magnitude squared coherence (MSC) is a traditional EEG–EMG coherence method, and its specific steps are as follows.

The Welch method [5,18] is used to separately segment the EEG signal and the EMG signal into L equal-length periods. After a spectral estimation is performed for each period, the estimation of the EEG–EMG coherence is computed with the MSC function. The estimation of the coherence [15,19] can be expressed by

$$CO_{xy}(f) = \frac{(1/L)\sum_{l=1}^{L} Y_l^*(f)X_l(f)}{\sqrt{(1/L)\sum_{l=1}^{L}|Y_l(f)|^2 \cdot (1/L)\sum_{l=1}^{L}|X_l(f)|^2}}, \tag{7}$$

where $\left|CO_{xy}(f)\right|^2$ is the estimation of the MSC function in the range of 0–1, $Y_l(f)$ represents the estimation of the spectrum of the EEG signal $y(n)$ in segment l, $X_l(f)$ represents the estimation of the spectrum of the EMG signal $x(n)$ in segment l, and * is the complex conjugate.

The computed values in the typical analytical method of MSC are generally low, which is not conducive to subsequent research and analysis. Eq. (7) can be utilized to compute the MSC of the EEG signal obtained by the abovementioned preprocessing approach and the EMG signal. Consequently, the estimation of the EEG–EMG coherence may reach 0.5 or higher.

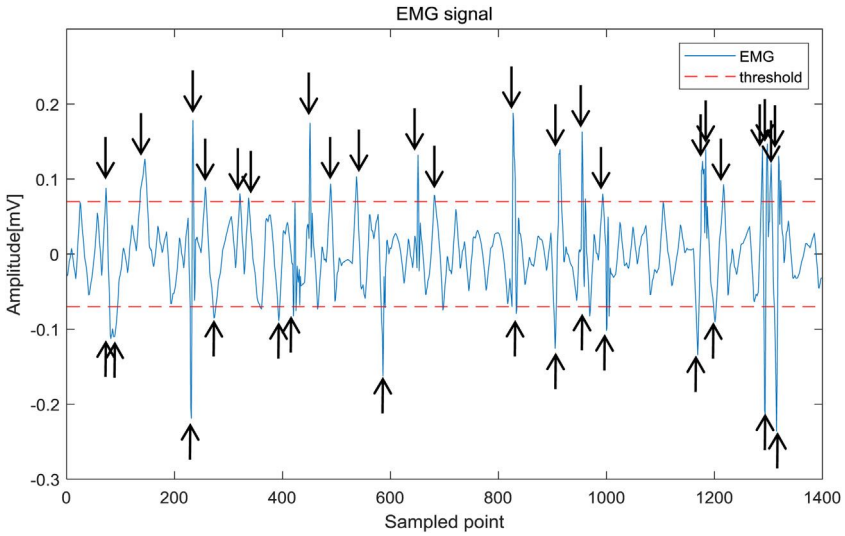

Fig. 2. Search for burst points in the EMG signal.

2.2.3. Wavelet coherence

MSC can only linearly estimate EEG and EMG signals. The wavelet coherence is used accordingly to analyze the enhanced EEG–EMG coherence, the aim of which is to depict its nonlinear characteristics.

Wavelet coherence renders the full use of wavelet transform characteristics and expands the signal to one in the time–frequency domain for analysis, which is important in handling nonstationary signals. Here, wavelet decomposition is used to decompose the preprocessed EEG signal into sub-signals of different frequency bands. The frequency bands (mainly the β-band and the γ-band) that control muscle movements are selected to perform wavelet coherence analysis with the EMG signal in the time–frequency domain.

We assume that there are two signal time series of $x(t)$ and $y(t)$ representing EMG and EEG respectively. The wavelet coefficients, denoted by $W_x(a, b)$, of the signal $x(t)$ are generated by convoluting the scaled wavelet function $\psi(t)$ with $x(t)$.

$$W_x(a, b) = \langle x, \psi_{a,b} \rangle = \frac{1}{\sqrt{a}} \int_{-\infty}^{\infty} x(t)\psi^*(\frac{t-b}{a})dt, \tag{8}$$

where a denotes the wavelet scale (a multiple of 2^j in general) and is inversely proportional to frequency, b is the smoothing parameter, t is the local time origin of the wavelet analysis, * is the conjugate, and $\psi(\frac{t-b}{a})$ represents the wavelet basis function. The Morlet wavelet [20] is selected in this study.

Torrence and Compo [21] defined the cross-wavelet transformation of $x(t)$ and $y(t)$ as $\left|W_{yx}(a, b)\right|$. Therefore, the wavelet cross-spectrum of the EEG signal $y(t)$ and the EMG signal $x(t)$ can be expressed as

$$|W_{yx}(a, b)| = |W_y(a, b)W_x{}^*(a, b)|. \tag{9}$$

The wavelet spectrum needs to be smoothened before the wavelet coherence is calculated to comprehensively obtain the synchronization information of the EEG and EMG signals. The smoothing function can further improve the signal after wavelet transformation, mainly by acting on the time and scale axes. The smoothing function is defined as

$$S(W) = S_a[S_t(W)], \tag{10}$$

where S_a denotes a smoothing operation on the scale axis, which is defined as $S_a(W(a, b)) = W(a, b)^* c_1 \Pi(0.6a)$, while S_t represents a smoothing operation on the time axis, which is defined as $S_t(W(a, b)) = W(a, b)^* c_2^{-\frac{t^2}{2a^2}}$. Here, c_1, c_2 represents the normalization coefficients that can be set to the value of 0.9, * represents a convolution calculation, and $\prod$ is a matrix function determined by the scale of the Morlet wavelet that can be set to the value of 0.6.

According to Torrence and Webster [22], wavelet coherence is defined as the absolute value of the normalized smooth cross-wavelet spectrum. Therefore, the wavelet coherence coefficient of $y(t)$ and $x(t)$ can be defined as follows [23]:

$$Wco_{yx}(a, b) = \frac{\left|S(W_{yx}(a, b))\right|}{\sqrt{S(\left|W_y(a, b)\right|^2)S(\left|W_x(a, b)\right|^2)}} \tag{11}$$

The wavelet coherence coefficient is in the range of 0–1. A value close to 0 indicates weak coherence, whereas a value close to 1 indicates strong coherence.

2.2.4. Coherence threshold evaluation

A coherence threshold evaluation method [24,25] is introduced to evaluate the statistical significance of the proposed coherence method. The computing formula is

$$CL = 1 - (1 - a)^{\frac{1}{L-1}} \tag{12}$$

where L represents the length of the data segments used for coherent analysis, α is the confidence level (usually set to 0.95), and CL stands for the confidence limit, also called the coherence threshold. If the computed coherence coefficients exceed the coherence threshold CL, then the EEG and EMG signals are significantly coherent. The EEG and EMG signals are not statistically coherent if the coefficients have values lower than the coherence threshold value.

The statistical differences of the EEG–EMG coherences under different conditions are quantitatively described in this study. The coherence significant area A_{coh}, which is depicted as the area beyond the significant coherence threshold CL and below the coherence curve, can be further expressed as

$$A_{coh} = \sum\nolimits_f \Delta f(\mathrm{Wco}(f) - CL) \tag{13}$$

where Δf represents the frequency resolution, f is the frequency of the calculated frequency band, and $W_{co}(f)$ is the coherence value higher than the significant coherence threshold CL value in f. The larger is the significant area A_{coh} of the EEG–EMG coherence, the more significant the coherence will be.

Fig. 3. The EEG and EMG acquisition.

2.3. Experimental scheme

The EEG data used in the experiment were collected by the SCAN 4.3 system of NeuroScan USA, whereas the EMG data were collected by the DELSYS Trigno™ wireless EMG system. Both data were sampled at 512 Hz. EEG was collected by setting the electrodes in the international 10–20 system standard. The reference electrodes were placed onto the subject's ears, and the C3 channel was selected for analysis. EMG was recorded using bipolar electrodes positioned over the subject's ulnar extensional wrist muscle (ECU), radial extension of the wrist muscle (ECR), and flexor digitorum (FD). Synchronous EEG and EMG data were recorded in three states, namely, hand fisting, wrist extension, and wrist flexion to investigate EEG–EMG coherence generated by different hand movements. Five healthy right-handed subjects (males, 23 ± 2 years old) were asked to perform the above actions. Fig. 3 shows the process of acquiring the EEG and EMG signals. All the subjects read and signed an informed consent form approved by an institutional review board.

The experimental processes were performed as follows. After resting for 10 s, each subject was instructed to clench his fist and keep this state for 5 s. EEG and EMG data were recorded at that time. Then, each subject was instructed to relax for 10 s, bend his wrist, and keep this state for 5 s. EEG and EMG data were recorded again at that time. Finally, after resting again for 10 s, each subject was asked to stretch his wrist and hold for 5 s. EEG and EMG data were recorded again at that time. Each step was repeated thrice. The experimental paradigm is shown in Fig. 4.

3. Results

3.1. EEG and EMG data

The succeeding discussions describe the enhanced EEG–EMG coherence results by taking the wrist flexion of a subject as the example. The EEG and EMG synchronization signals recorded in the experiment are subjected to wavelet threshold denoising. Subsequently, the EMG signals of ECU, ECR, and FD are obtained, as shown in Fig. 5.

Fig. 6 shows the denoised EEG signals of the C3 channel obtained on the basis of the wrist flexion. The EMG signals of ECU, ECR, and FD in Fig. 4 can be selected for the enhanced EEG–EMG coherence analysis. The denoised EEG signal of the C3 channel is sampled, averaged, resampled and reassembled according to the burst points of the abovementioned three channels EMG signals respectively and the preprocessed EEG signals are obtained (Fig. 6).

The classic Walter classification method [26,27] can be used to divide the EEG signal into five functional frequency bands according to frequency: δ-band (1–4 Hz), θ-band (4–8 Hz), α-band (8–14 Hz), β-band (14–30 Hz), and γ-band (30–50 Hz). Many studies have reported that the EEG–EMG coherence of the autonomous hand movements of healthy people is prominent in the β- and γ-bands [1,28]; by contrast, the prominent EEG–EMG coherence in the α-band and at the lower frequencies is often regarded as the characteristic of patients with pathological tremors and usually absent among healthy people [29]. Therefore, the present study focuses on the analysis of EEG–EMG coherence in the β- and γ-bands under autonomous hand movements.

3.2. MSC processing

The MSCs of the EEG signal (from the advanced preprocessing) and the EMG signal (with the part of the EEG signal in the frequency range of 0–60 Hz) are computed to obtain the EEG–EMG coherence curves under the three actions of wrist flexion, wrist extension, and hand fisting. At the same time, the original coherence curves are drawn for comparison, as shown in the left sides of Figs. 7–9. Furthermore, the coupling degrees between EEG and EMG signals generated by different autonomous hand movements are quantitative analyzed. The corresponding significant coherence areas in the β- and γ-bands are computed according to Eq. (13), as shown in the right sides of Figs. 7–9.

The results shown in Figs. 7(a), 8(a), and 9(a) indicate that the original MSCs are much weaker than the enhanced MSCs in general. Under the movements of wrist flexion, wrist extension, and hand fisting, the significant coherences of the original MSCs are at their maximum at 0.048, 0.05, and 0.07, whereas the enhanced MSC significant coherence peak points have reached 0.59, 0.68, and 0.75, respectively.

The area in which the original MSC coefficients exceed the threshold CL is relatively small, indicating a coherence degree that are generally non-obvious. After performing the enhancement operation, the overall MSC coefficients are improved substantially, and the significant coherence area is increased, which renders it conducive for coherence analysis. This finding can be distinctly seen in Figs. 7(b), 8(b), and 9(b).

Some conclusions from the enhanced coherence analysis graph can be drawn. The comparisons of A_{coh} between the β-band and the γ-band under different hand movements indicate significant coherences, particularly in the β-band when wrist flexion or wrist extension occurs, unlike in the γ-band. Some differences between wrist flexion and wrist extension in the significant coherence area can be attributed to the implemented coherence frequency ranges and peaks. The coherence frequency range at 16–24 Hz of the wrist extension is larger than that of the wrist flexion at 22–26 Hz. This phenomenon may be related to the number of times in which muscles are used in daily life. People use wrist flexor muscles, such

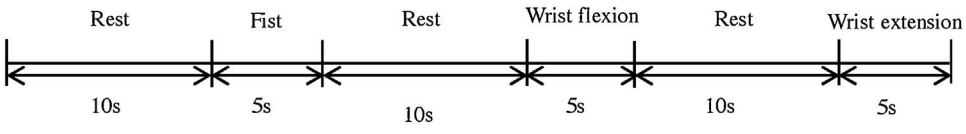

Fig. 4. Experimental paradigm.

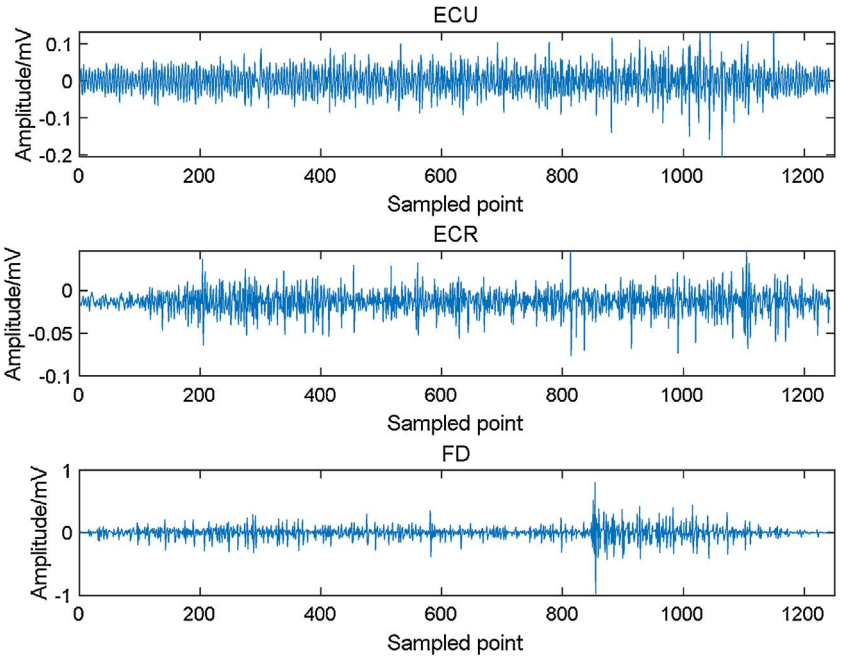

Fig. 5. Denoised EMG signal (Wrist flexion).

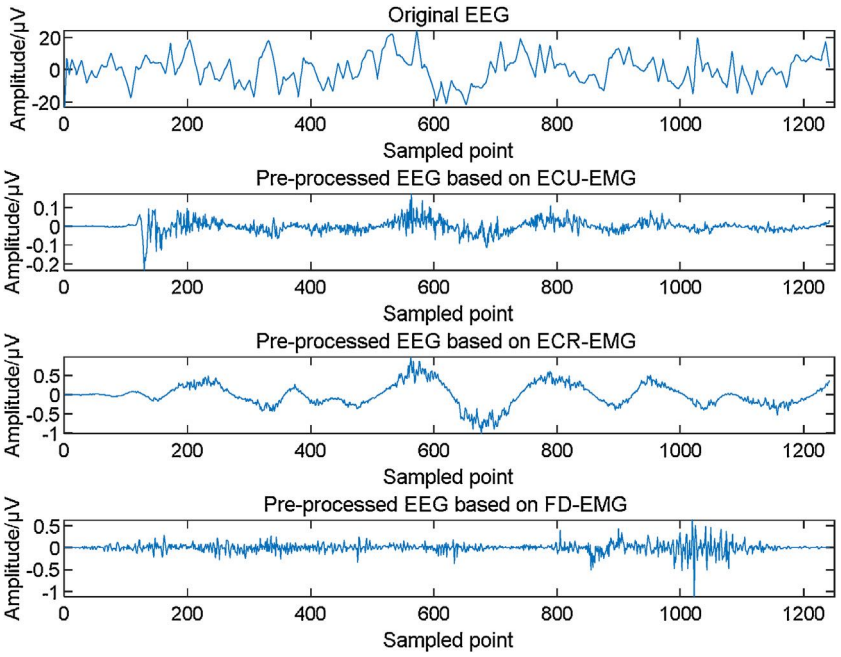

Fig. 6. Original EEG signal and preprocessed EEG signals (wrist flexion).

as when grasping objects, more frequently than wrist extensor muscles, indicating the long-term adaptability of the former [30]. Therefore, the resources integrated and synchronized by the brain are low when completing wrist flexion, which is represented in this study as having relatively narrow coherence frequency bands and low peaks. Moreover, wrist extensor muscles are seldom used, and the brain needs to integrate and synchronize much more resources when wrist extension is completed, indicating relatively wide coherence frequency bands and high peaks. As for the hand fisting, the significant coherent area is concentrated at 20–30 Hz in general, and the peak occurs mainly in the β-band.

The wrist flexion, wrist extension, and hand fisting case designs in this study have significant coherences in the β-band, indicating that the nerve impulses of the cortex and the spinal cord mainly oscillate in this frequency band. This phenomenon drives the autonomous movement of the body. The significant coherence areas of the different myoelectrical lead points in the β-band are contrasted. The results indicate that the nerves innervating the active muscles are more strongly associated with cortical functions compared with the other nerve types.

3.3. Wavelet coherence processing

On the basis of the above findings, EEG–EMG wavelet coherence can be performed by selecting the active muscles that dominate the movements. Subsequently, C3-ECU is selected with wrist flexion,

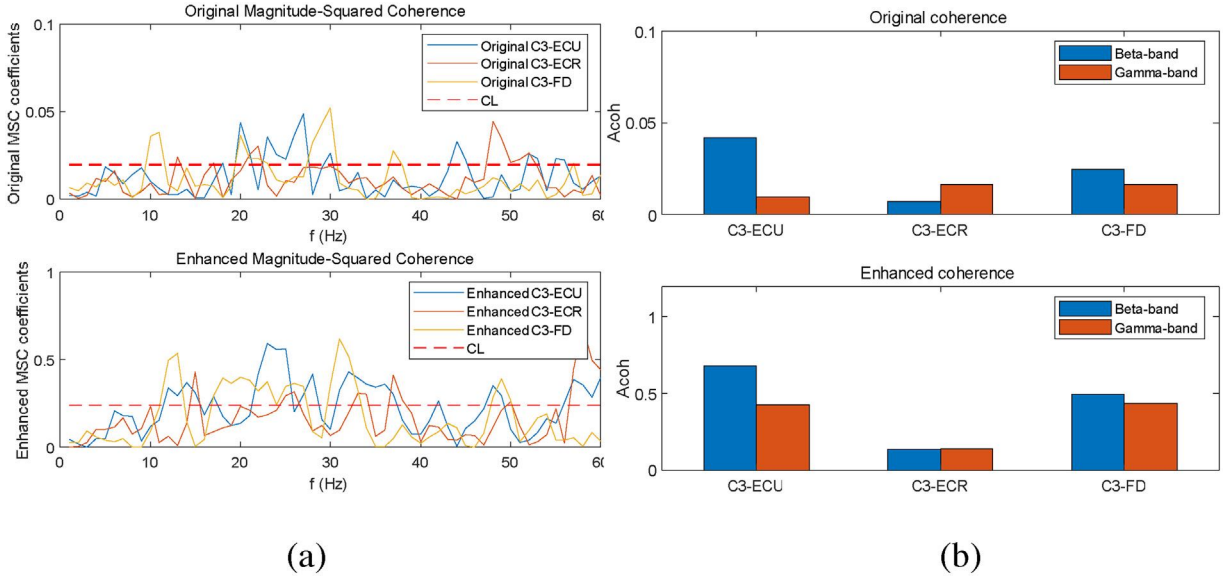

Fig. 7. Comparison before and after enhancements (wrist flexion): (a) MSC curves, (b) significant coherence areas in the β- and γ-bands.

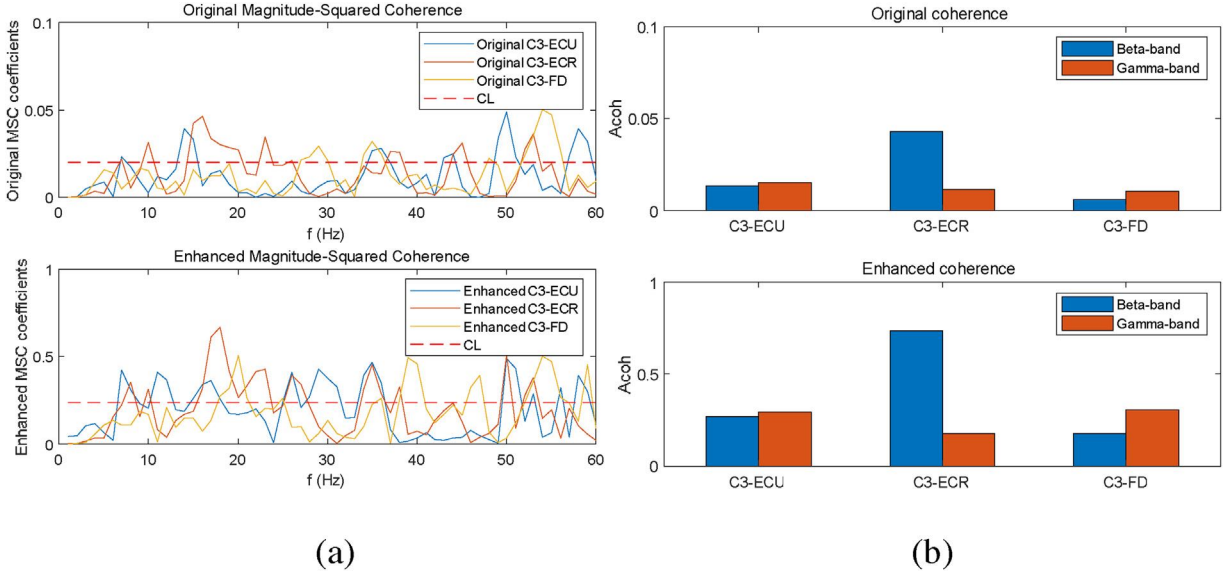

Fig. 8. Comparison before and after enhancements (wrist extension): (a) MSC curves, (b) significant coherence areas in the β- and γ-bands.

C3-ECR is selected with wrist extension, and C3-FD is selected with the hand fisting. The EMG signals and the advanced preprocessed EEG signals are used to compute the wavelet coherence, and the time–frequency diagrams of the wavelet coherence coefficients, as shown in Figs. 10–12, are obtained.

The yellow areas in the right parts of Figs. 10–12 are much larger than those in the left parts. The differences represent the EEG–EMG coherence coefficients after undergoing advanced preprocessing, in which the values are substantially increased relative to the original EEG–EMG coherence estimations. The result further validates the feasibility of the proposed method for enhancing EEG–EMG coherence.

In addition, as shown by the right parts of Figs. 10–12, the most relevant areas of EEG and EMG are generally in the frequency ranges of 4–35 Hz, 14–40 Hz, and 22–64 Hz, which correspond to wrist flexion, wrist extension, and hand fisting, respectively. However, the most significant coherence frequency bands of the original time–frequency diagrams are somewhat difficult to determine, particularly because the values of the original coherence coefficients are very small. These observations further demonstrate the convenience of analyzing EEG–EMG coherence in daily autonomous movements.

The original time–frequency diagrams in the left parts of Figs. 10–12 cannot embody the coherence variations of the different hand movements; hence, the enhanced coherence time–frequency diagrams are analyzed. The areas of EEG–EMG coherence where coherence coefficients exceed 0.75 differ among the three hand movements. The largest is the area of the wrist extension, followed by the area of the hand fisting, and finally by the area of the wrist flexion. This difference corresponds to the discussion on the adaptability of using hand movements in daily life.

3.4. Hand movements recognition

Furthermore, to validate the rationality of the proposed method, we will try to distinguish different hand movements by extracting

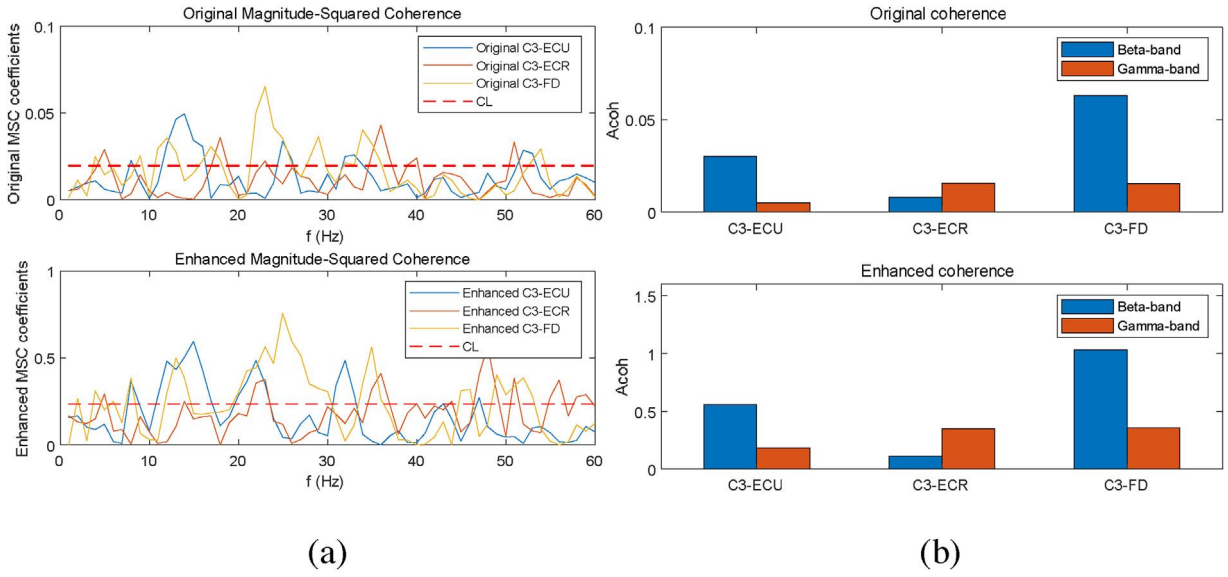

Fig. 9. Comparison before and after enhancement (hand fisting): (a) MSC curves, (b) significant coherence areas in the β- and γ-bands.

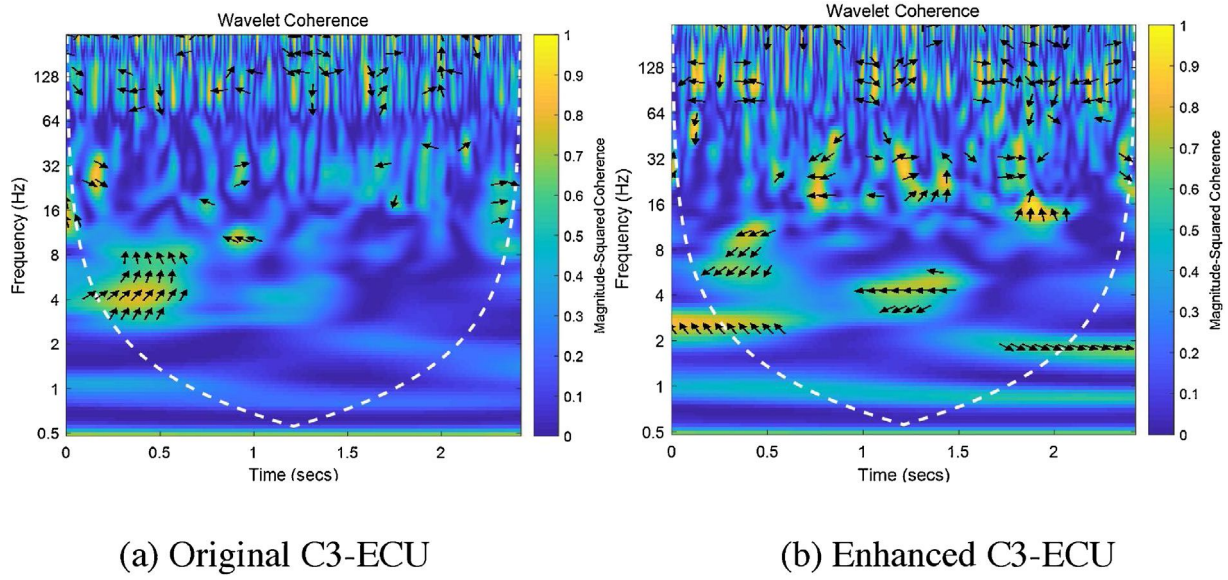

Fig. 10. Wavelet coherence coefficient time–frequency diagram (wrist flexion).

features related to the enhanced MSC. Here, we adopt SVM method to identify different hand movements. The data obtained from five subjects in the above experiment were analyzed.

It cannot be ignored that the selection of features aiming at hand movements have deeply influenced the classification results in this study. Based on the above coherence analysis, the coherence of the β-band and the γ-band is more significant in the hand movements. Therefore, we computed the MSC coefficients averaged in β-band and in γ-band, respectively, among three different cortico-muscular combinations of C3-ECR, C3-ECU and C3-FD. Then the MSC 3×2 vector was obtained and chosen as the features vector for classification analysis. Subsequently, the MSC features vector was fed to the SVM classifier for training and testing in 10-fold cross-validation way.

Table 1 shows the classification mean accuracy rate before and after the enhancement of EEG-EMG coherence estimation. It can be seen that the mean accuracy rate of the original MSC is 79.33%, whereas the mean accuracy of the enhanced MSC has reached 83.50%. This result reveals that the enhanced MSC coefficients can still reflect the characteristics of different hand movements correctly, and validate the reliability of our proposed method. Moreover, after enhancing MSC coefficients, the classification accuracy is improved, which sheds light on how the cortex controls muscles to some extent. And it also is indicated that the proposed method has great potential for the recognition of human motion intentions and is worthy of our future study.

Table 1
Comparison of mean accuracy rate.

	Original MSC	Enhanced MSC
SVM-mean accuracy rate	79.33%	83.50%

4. Conclusion and discussion

The traditional estimation of EEG–EMG coherence generated by common hand movements is hindered by extremely low val-

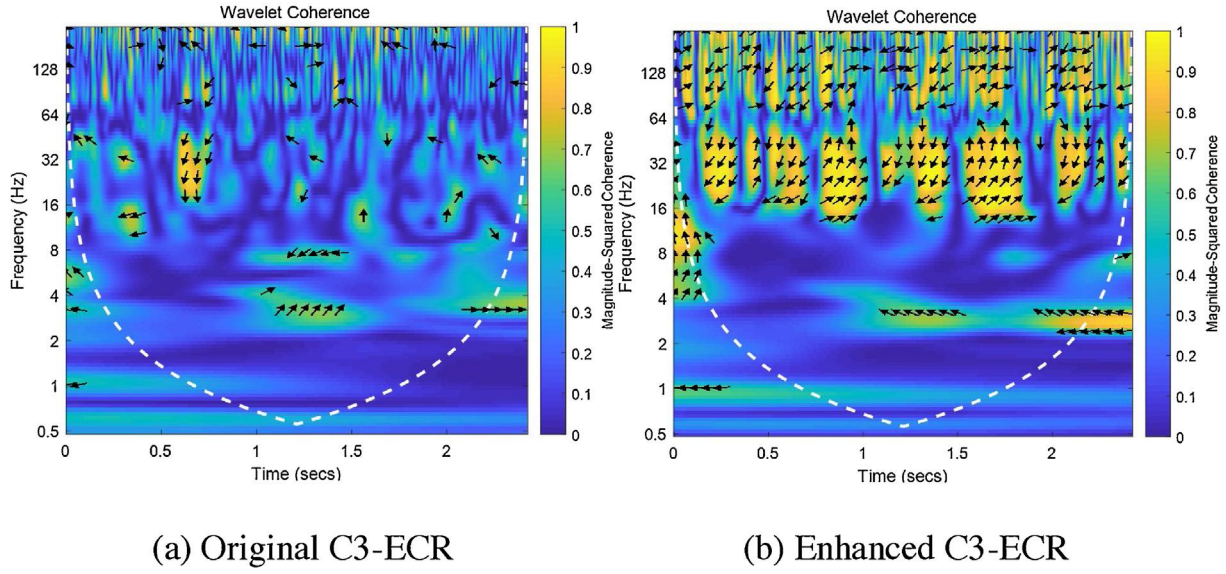

Fig. 11. Wavelet coherence coefficient time–frequency diagram (wrist extension).

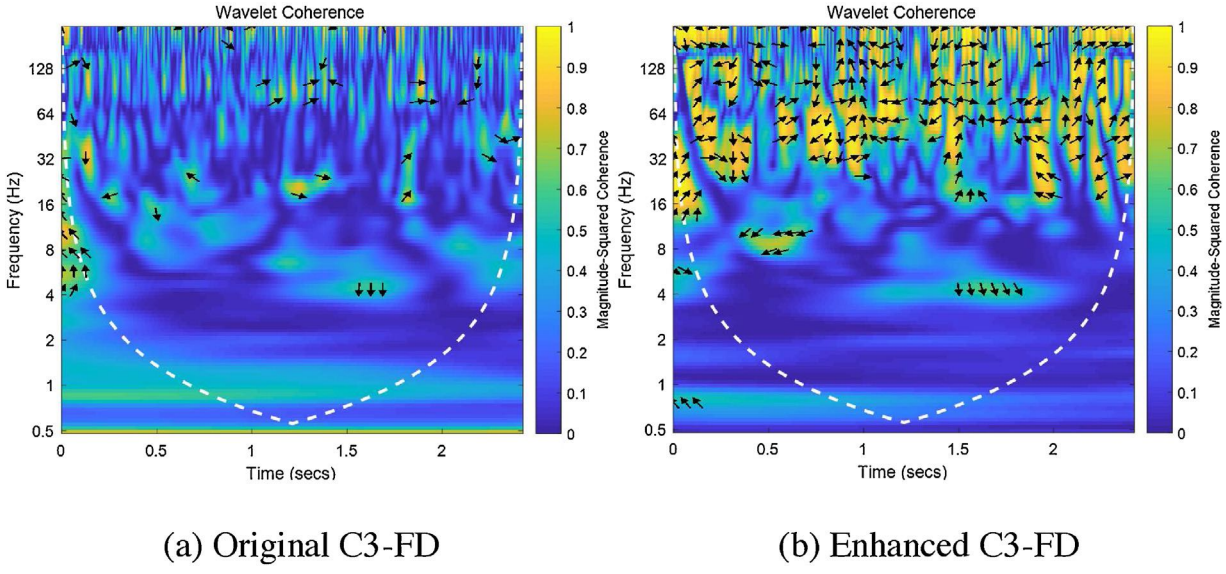

Fig. 12. Wavelet coherence coefficient time–frequency diagram (hand fisting).

ues and thus cannot be comprehensively analyzed. The present study proposes a method to extract the EEG signal based on the burst pulse points of the EMG signal: the denoised EEG signal is sampled by multiplying normalized synchronous EMG signal and a Hamming window slides along the sampled EEG signal to obtain a moving average (MA) EEG; then MA EEG is resampled again and reassembled, resulting in the advanced preprocessing approaches. In this manner, the most useful EEG signal, which is the most relevant to the EMG signal generated by the different hand movements of wrist flexion, wrist extension, and hand fisting, can be obtained. Then, the coherence is analyzed by using the MSC and wavelet coherence methods. The compared experimental results of the estimation of the coherence between the EEG signal (before and after advanced preprocessing) and the EMG signal indicates that the proposed method can significantly enhance the coherence between EEG and EMG signals. Moreover, the proposed method is more conducive in analyzing EEG–EMG coherence generated by different autonomous movements than by using the traditional method. The results of the enhanced MSC show that EEG–EMG coherence generated by autonomous motion is mainly concentrated in the β-band (14–30 Hz). The differences are more apparent in the EEG–EMG coherence of the wrist flexion than that of the wrist extension, and they correspond to the coherence peaks and ranges of the frequency bands. Then, the results of the wavelet coherence also indicate the effective enhancement of EEG–EMG coherence.

The advantages of adopting the proposed enhanced method are associated with the study results, which emphasize EEG–EMG coherence based on the premise of ensuring correctness. In particular, the coherence coefficients obtained in this study are much larger than the original ones. However, the present research is limited by the rarity of the selected subjects, movements and channels used for collecting EEG/EMG and the appropriateness of selecting parameters (the selection of parameters for advanced preprocessing needs substantial research experience). Besides, the proposed method is applicable to the coherent analysis of EEG and EMG signals collected only at the same frequency, and further improvement may be necessary at different frequencies. Moreover, all subjects in

this study are healthy, and whether the proposed method is effective for people with movement disorders or cognitive impairment remains to be studied. These research aspects need to be further investigated to address abovementioned limitations and achieve comprehensively appropriate results.

The prediction of the limb movement intention using the enhanced MSC should be studied in a future work. The construction of a cortex-muscle functional network using the proposed method, which maybe further reflect the functional connection between the cortex and the muscle, is qualified to be a decent work in the future. These research studies have tremendous potential for revealing the mechanism about how nerves control muscles.

Acknowledgements

This work was supported by the National Natural Science Foundation of China (Nos. 61971169, 61671197, 61673350 and 60903084), Zhejiang Public Welfare Technology Research (No. LGF18F010006) and Jinhua Science and Technology Research Project (No. 2019-3-020).

Declaration of Competing Interest

The authors declare that they have no known competing financial interests or personal relationships that could have appeared to influence the work reported in this paper.

References

[1] J. Gwin, D. Ferris, Beta- and gamma-range human lower limb corticomuscular coherence, Front. Hum. Neurosci. 6 (2012) 258, http://dx.doi.org/10.3389/fnhum.2012.00258.
[2] L. Patino, W. Omlor, V. Chakarov, M.-C. Hepp-Reymond, R. Kristeva, Absence of gamma-range corticomuscular coherence during dynamic force in a deafferented patient, J. Neurophysiol. 99 (4) (2008) 1906–1916, 2008/04/01.
[3] C. Braun, M. Staudt, C. Schmitt, H. Preissl, N. Birbaumer, C. Gerloff, Crossed cortico-spinal motor control after capsular stroke, Eur. J. Neurosci. 25 (9) (2007) 2935–2945, 2007/05/01.
[4] L.V. Schaefer, F.N. Bittmann, Coherent behavior of neuromuscular oscillations between isometrically interacting subjects: experimental study utilizing wavelet coherence analysis of mechanomyographic and mechanotendographic signals, Sci. Rep. 8 (1) (2018), 15456, 2018/10/18.
[5] M. Muthuraman, A. Galka, G. Deuschl, U. Heute, J. Raethjen, Dynamical correlation of non-stationary signals in time domain—a comparative study, Biomed. Signal Process. Control 5 (3) (2010) 205–213, 2010/07/01/.
[6] F. He, et al., Nonlinear interactions in the thalamocortical loop in essential tremor: a model-based frequency domain analysis, Neuroscience 324 (2016) 377–389, 2016/06/02/.
[7] M. Fauvet, S. Cremoux, A. Chalard, J. Tisseyre, D. Gasq, D. Amarantini, A novel method to generalize time-frequency coherence analysis between EEG or EMG signals during repetitive trials with high intra-subject variability in duration, 2019 9th International IEEE/EMBS Conference on Neural Engineering (NER) (2019) 437–440.
[8] S. Roopa, S.V. Narasimhan, Magnitude square coherence (MSC) estimation via an ARMA model based on analytic DCT and group delay, Circuits Syst. Signal Process. 37 (3) (2018) 1203–1222, 2018/03/01.
[9] A. Chowdhury, H. Raza, Y.K. Meena, A. Dutta, G. Prasad, An EEG-EMG correlation-based brain-computer interface for hand orthosis supported neuro-rehabilitation, J. Neurosci. Methods 312 (2019) 1–11.
[10] F.A. Mahdavi, S.A. Ahmad, M.H. Marhaban, M.-R. Akbarzadeh-T, Surface electromyography feature extraction based on wavelet transform, Int. J. Integr. Eng. 4 (3) (2012).
[11] C. Ieracitano, J. Duun-Henriksen, N. Mammone, F.L. Foresta, F.C. Morabito, Wavelet coherence-based clustering of EEG signals to estimate the brain connectivity in absence epileptic patients, International Joint Conference on Neural Networks (2017).
[12] Y. Zhang, S.N. Chang, G. Zhou, J. Jin, A. Cichocki, Temporally constrained sparse group spatial patterns for motor imagery BCI, IEEE Trans. Cybern. (99) (2018) 1–11, vol. PP.
[13] Z. Jin, G. Zhou, D. Gao, Y. Zhang, EEG classification using sparse Bayesian extreme learning machine for brain–computer interface, Neural Comput. Appl. (2018) 1–9.
[14] Y. Jiao, et al., Sparse group representation model for motor imagery EEG classification, IEEE J. Biomed. Health Inform. 23 (2) (2018) 631–641.
[15] R. Bortel, P. Sovka, EEG–EMG coherence enhancement, Signal Process. 86 (7) (2006) 1737–1751.
[16] X. Xi, M. Tang, S.M. Miran, Z. Luo, Evaluation of feature extraction and recognition for activity monitoring and fall detection based on wearable sEMG sensors, Sensors (Basel) 17 (6) (2017), May 27.
[17] V.M. McClelland, Z. Cvetkovic, K.R. Mills, Rectification of the EMG is an unnecessary and inappropriate step in the calculation of Corticomuscular coherence, J. Neurosci. Methods 205 (1) (2012) 190–201, Mar 30.
[18] S. Goel, G. Kaur, P. Tomar, Performance analysis of Welch and Blackman Nuttall window for noise reduction of ECG, 2015 International Conference on Signal Processing, Computing and Control (ISPCC) (2015) 87–91.
[19] D. Tuncel, A. Dizibuyuk, M.K. Kiymik, Time frequency based coherence analysis between EEG and EMG activities in fatigue duration, J. Med. Syst. 34 (2) (2010) 131–138, 2010/04/01.
[20] J. Kopal, O. Vyšata, J. Burian, M. Schätz, A. Procházka, M. Vališ, Complex continuous wavelet coherence for EEG microstates detection in insight and calm meditation, Conscious. Cogn. 30 (2014) 13–23, 2014/11/01/.
[21] C. Torrence, G.P. Compo, A practical guide to wavelet analysis, Bull. Am. Meteorol. Soc. 79 (1) (1998) 61–78.
[22] C. Torrence, P.J. Webster, Interdecadal changes in the ENSO–monsoon system, J. Clim. 12 (8) (1999) 2679–2690.
[23] J.-P. Lachaux, et al., Estimating the time-course of coherence between single-trial brain signals: an introduction to wavelet coherence, Neurophysiol. Clin. Neurophysiol. 32 (3) (2002) 157–174, 2002/06/01/.
[24] A. Ritterband-Rosenbaum, et al., A critical period of corticomuscular and EMG–EMG coherence detection in healthy infants aged 9–25 weeks, J. Physiol. 595 (8) (2017) 2699–2713.
[25] T. Ushijima, A. Sahroni, T. Igasaki, N. Murayama, Time-lapse changes in EEG-EMG coherence during weak voluntary contraction of the tibialis anterior muscle, 2017 10th Biomedical Engineering International Conference (BMEiCON) (2017) 1–5.
[26] E. Kirino, S. Tanaka, M. Fukuta, R. Inami, R. Inoue, S. Aoki, Functional connectivity of the caudate in schizophrenia evaluated with simultaneous resting-state functional MRI and electroencephalography recordings, Neuropsychobiology 77 (4) (2019) 165–175.
[27] T. Mima, T. Matsuoka, M. Hallett, Functional coupling of human right and left cortical motor areas demonstrated with partial coherence analysis, Neurosci. Lett. 287 (2) (2000) 93–96, 2000/06/23/.
[28] S.N. Baker, E. Olivier, R.N. Lemon, Coherent oscillations in monkey motor cortex and hand muscle EMG show task-dependent modulation, J. Physiol. 501 (1) (1997) 225–241, 1997/05/01.
[29] F. Budini, et al., Alpha band cortico-muscular coherence occurs in healthy individuals during mechanically-induced tremor, PLoS One 9 (12) (2014), e115012.
[30] K. Salonikidis, I.G. Amiridis, N. Oxyzoglou, P. Giagazoglou, G. Akrivopoulou, Wrist flexors are steadier than extensors, Int. J. Sports Med. 32 (10) (2011) 754–760, //26.09.2011.